Rotational Sequences of Global Oscillations inside the Sun

Charles L. Wolff

NASA Goddard Space Flight Center, Greenbelt, MD 20771

charles.wolff@gsfc.nasa.gov

Rotational Sequences of Global Oscillations inside the Sun

by Charles Wolff

POPULAR SUMMARY

Many oscillation modes can exist inside the Sun and cover the entire globe. The most fundamental are modes trapped below the convective layers (i. e., below the outer 30% of a solar radius). These modes engage most of the Sun's mass in organized motion and affect the deepest layers where its energy is generated. Beat periods between the rotation rates of the various modes can be many month to years. When the longer beat periods modulate solar luminosity, they become potentially interesting to the Earth climate problem.

In this paper, I found clear evidence for the rotation rates of both gravity modes and Rossby modes. This proves they are excited in the Sun. There was also strong evidence for beat periods between the gravity modes. (Astronomers call these "g-modes" and "r-modes". The Rossby waves of meteorology are just local approximations to the Rossby modes of a sphere.)

All the low angular harmonic modes were detected--from #2 up to #7--by means of a very simple mathematical sequence which their rotation rates have to obey. Some additional modes up to #14 were also seen. Beyond that number, the observations do not have enough resolving power to reveal any higher modes.

The observations used were the 54 year data set of daily measurements of thermal radio flux from the Sun. This rises and falls with other popular measures of solar variability such as the sunspot number and solar irradiance, so similar results would be expected if one of these data sets had been used.

We learn two other things about the inside of the Sun in addition to detecting that the oscillations exist. The Sun's average interior rotation period is measured to be 29.1 days, apparent from Earth. This is longer than the well known 27 day surface rotation period at low latitudes. Secondly, the 29.1 day period and theoretical properties of the modes require that the wave energy of the global modes is being reflected very deep in the Sun but not from the very center. The reflection layer is at 18% of the solar radius, which happens to be the same place where others have already measured a pronounced anomaly in sound speed. Something major is happening at 18% of the solar radius that theoreticians have yet to explain.

ABSTRACT

A very simple mathematical sequence is detected in a half century of thermal radio flux from the Sun. Since the only known physical cause of the sequence is global oscillations trapped in the nonconvecting solar interior, g-modes and probably r-modes are active. If so, their rotation frequencies are detected and some previously reported difference frequencies are confirmed with high confidence. All angular harmonics for $2 \leqslant \ell \leqslant 7$ are detected as well as some others up to the limit $\ell \leqslant 14$ resolvable by the observations (a Fourier spectrum of the 10.7 cm flux time series). The mean sidereal rotation of the nonconvecting interior is 428.2 nHz as averaged by g-modes and 429.8 nHz by the r-modes, indicating that g-mode energy is a bit more centrally concentrated. Helioseismology measures such rotation rates near 0.36R (R = solar radius), so the global modes would have about half their kinetic energy above and below that level. This, and the known log(r) energy dependence of most modes implies that these oscillations are significantly reflected near 0.18R, the same level at which sound speed measurements display a maximum departure from theoretical models.

Subject headings: Sun: oscillations—Stars: oscillations—Sun: activity—Sun: interior

1. INTRODUCTION

Linear oscillation modes $\xi(\mathbf{r})e^{i\sigma t}$ trapped in stellar layers that rotate slowly at constant rate Ω are well understood (Cox 1980; Unno, *et al.* 1989). In co-rotating coordinates, the oscillation frequency σ and spatial variation,

$$\xi = \hat{\mathbf{r}} f_1 Y + r f_2 \nabla Y - f_3 \mathbf{r} \times \nabla Y, \tag{1}$$

depend on the radial and angular harmonic numbers (n, ℓ, m), spherical harmonic functions $Y = Y_\ell^m(\theta, \phi)$, and the radial eigenfunctions $f_i(r)$. Only one Y_ℓ^m is needed to describe the dominant part of the motion which is consequently a running wave in longitude, $\exp[i(m\phi + \sigma t)]$. For r-modes the Coriolis force and f_3 term dominate (Provost, Berthomieu, & Rocca 1981; Smeyers, Craeynest, & Martens 1981). For g-modes, buoyancy is the main force and the f_3 term is neglected (Cowling 1941). Christensen-Dalsgaard & Berthomieu (1991) reviewed g-mode properties and Wolff (2000) the r-modes.

To first order, most g-modes and low radial harmonic r-modes have rotational properties that are particularly simple for standing modes (§2), the subject of this paper. This signature of their presence (eq. [2]) gives strict tests to apply to observations. Both g- and r-modes would be trapped in the nonconvecting solar interior which rotates like a solid body with only a few percent deviation (Eff-Darwich, Korzennik, & Jimenez-Reyes 2002). This justifies using theory based on uniform rotation for early searches for the rotational signature. In §3, the signature is detected with high confidence in three different parts of the 10.7 cm flux spectrum.

2. ROTATION OF GLOBAL MODES

For r-modes, a point of constant phase drifts backward relative to a rotating stellar fluid. But relative to inertial space the mode turns forward at the rate (Saio 1982)

$$\nu_\ell = \nu_s - \frac{\nu_d}{\ell(\ell+1)}. \tag{2}$$

where $\nu_s = \Omega/2\pi$ is the fluid rotation rate in Hertz and the drift constant $\nu_d = 2\nu_s$ for r-modes. Since this is independent of m, the standing r-mode (sum of the +m and –m mode) rotates at the same rate. The inertial rotation of a standing g-mode is also given by equation (2) but now (Wolff 1974) $\nu_d = \nu_s J/K$ from the classic solution of Ledoux (1951)

where $J = \int dm(2f_1 f_2 + f_2^2)$, $K = \int dm[{f_2}^2 + {f_1}^2/\ell(\ell+1)]$, $dm = 4\pi r^2 \rho dr$, and ρ is the density. Asymptotic g-modes ($n^2 >> \ell^2$) have J/K = 1 but, for other g-modes, J/K must be computed.

A standard solar model was used (Guenther, *et al.* 1992) with its buoyancy frequency (Brunt-Vaisala) arbitrarily reduced for $r < 0.21R$ until reaching zero at r = 0.15R (R = solar radius). This simulates the main effect on these oscillations of an assumed partial mixing near 0.18R where sound speed measurements show a persistent discrepancy with interior models (Basu *et al.* 2000; Kosovichev *et al.* 1997). The steeply declining buoyancy frequency excludes oscillation energy from the inner core where most radiative damping would occur, making g-mode excitation more likely. Many have discussed mixing part or all of the core, e. g., Richard & Vauclair (1997); Brun, Turck-Chieze, & Morel (1998). A sampling of g-mode solutions was computed and the resulting values of J/K are shown in table 1. Their departure from unity (the asymptotic case) closely follows the empirical formula

$$J/K = 1 - 0.45(\ell^*/n)^{3/2} \tag{3}$$

where $\ell^* = [\ell(\ell+1)]^{1/2}$. Oscillations trapped between 0.18R and the convective envelope, 0.713R, will have equal kinetic energy above and below the logarithmic midpoint, since energy is distributed closely proportional to log(r) for most g-modes in the Sun (Wolff 1979) and also for r-modes. At this midpoint, 0.358R, the Sun's sidereal rotation is 429 ± 2 nHz from the curves given by Eff-Darwich, Korzennik, & Jimenez-Reyes (2002). The rate has a slight positive slope with radius. Since the effective rotation sensed by an oscillation is the energy-weighted mean, ν_s in equation (2) should be close to 429 nHz.

3. ROTATIONAL SIGNATURES IN SOLAR ACTIVITY

The 10.7 cm Radio Flux Index F_{10} is available at www.drao.nrc.ca/icarus/www from Dominion Observatory. The $\approxeq$ 20,000 daily values from 1947 Mar 5 through 2001 Nov 18 were compressed to about 4000 by taking 5 day averages. This widely used index varies with the 11 year cycle and the monthly rotation. Any true frequency ν_t influencing the index appears in the Fourier spectrum with aliases $\nu_t \pm i\nu_m$ where i is a small integer and modulating frequencies ν_m are (11 yr)$^{-1}$, (1 month)$^{-1}$, and any other strong modulator. This clutters the spectrum with many lines that look like noise. To reduce long period aliases, the deviation from the running mean $\bar{F}$—a one year boxcar average—was used.

Figure 1a shows the Fourier spectrum of $(F_{10} - \bar{F})\bar{F}^{-2}$. The decline below 30 nHz is not solar but is due to subtracting $\bar{F}$. The feature between 400 and 470 nHz is sometimes loosely attributed to active regions rotating across the disk but the fastest such rate apparent from Earth is 435 nHz. At least part of this bulge is unexplained. The rise in amplitude below 60 nHz may be due to overlapping sequences of beats between g-mode rotation rates mostly following equation (2) (Wolff (1983), hereafter "paper I"). The one beat sequence in that paper that overlaps no other is strongly confirmed on Figure 1b by the relevant part of the F_{10} spectrum. Vertical lines mark the differences between the ℓ = 2 case and the other frequencies in table 1 of paper I, extended for $\ell > 11$ using the same equation. These theoretical lines are rotational beat frequencies. They mostly hit tall lines in the F_{10} spectrum and every line for $\ell \leqslant 8$ is detected. Anyone assuming that the observed spectrum is mostly noise bears the heavy burden of explaining why the same theoretical sequence is detected in both F_{10} (Fig. 1b) and in sunspots (paper I) when only 25% of the latter data is contemporaneous with the former. Noise doesn't behave that way.

The well known binomial expression

$$P(n,k) = \frac{n!}{k!(n-k)!} p^k (1-p)^{n-k} \tag{4}$$

gives the probability P that k frequencies out of a total group of n will accidentally agree with observation if p is the probability that any random frequency agrees. To use this we need a success criterion for which p is a constant. The dashed curve, 1.2M, on every figure is based on M—a 20 nHz wide running mean of the spectrum. It turns out that 32.4% of the spectral points lie above this curve in any broad segment of the spectrum. By taking the dashed curve as the threshold for detection, one can use p = 0.324 everywhere. Of the 12 resolvable lines on Figure 1b, nine hit the spectrum above this curve making P(12, 9) = 0.0027, which is an impressive 3σ detection of the beat sequence.

When applying equation (2) to g-modes, $\nu_d = 381$ nHz as determined in paper I which stated it more generally as (762 nHz)/S where S (= 1 or 2) is the rotational symmetry of the modes. In all subsequent work, S = 2 has been used, meaning that a family of g-modes for a given ℓ has two hot longitudes, 180° apart at low latitudes (Wolff 1974). Thus, $2(\nu_\ell - \nu_2)$ are the expected beat frequencies with the $\ell = 2$ g-mode, including the small deviations measured in paper I for $\ell \leqslant 3$. Finally, note that ν_s cancels from the difference frequencies so paper I actually measured ν_d and not the stellar rotation rate.

In a sufficiently long data set, the rate at which a hot g-mode longitude faces Earth, $2(\nu_\ell - 31.69$ nHz), should also appear. These lines should be weaker than the beats since detectible change at the surface is likely only after some area at the base of the convection zone has been heated enough to stimulate an overturning. Beats do this better since two or more modes are contributing at the same location. Searching close to the expected 429 nHz (see end of §2), I found that equation (2) with $\nu_s = 428.2$ nHz fits the spectrum. Figures 1c and 1d mark these g-mode rates. Of the 13 predicted lines resolvable by the data, 8 hit the spectrum above the dashed curve. Since a free parameter (ν_s) always allows one

observed line to be matched, I discarded one successful line from the sample obtaining P(12, 7) = 0.042. This 2σ confidence level lends support to the above 3σ detection of the same sequence by the beat frequencies. The overall probability that agreement on figure 1 is accidental is P(12+12, 9+7) = 5 x 10^{-4}.

The r-modes assist convection not with heat but by supplying vorticity and a zonal velocity gradient. This mechanism, reinforced by the $\ell = 1$ mode, favors the synodic frequencies, ν_ℓ – 31.69 nHz, which are shown on figure 2 using ν_s = 429.8 nHz in equation (2). Nine of the 13 lines are detected including all for $\ell \leqslant 7$. Again discarding one successful line gives an accidental probability, P(12, 8) = 0.013, which is a $2\frac{1}{2}\sigma$ detection even without correcting for the interference at $\ell = 9$ and possibly $\ell = 8$ from the dotted triplet. (Closely spaced lines can either depress the spectrum if out of phase or enhance it if in phase.) The triplets are centered on the sidereal rates ν_ℓ. Evidence that these are aliased into at least triplets as they beat with the $\ell = 1$ modes will be discussed elsewhere. Wolff & Hoegy (1989) suggested 1.5 nHz for such a rate and that is the splitting drawn on Figure 2.

4. SUMMARY AND IMPLICATIONS

Few realize how hard it is to fit data with a large number of rates from equation (2) having only one free parameter, ν_s. (ν_d was already known from theory for r-modes and from earlier work for g-modes.) The g-mode sequence was detected with especially high confidence: accidental probability, 5 x 10^{-4}. Unfortunately, seeing high confidence levels has little impact existing opinions. But it must strain belief that we have been uncommonly lucky four times (!) with the same sequence (figs. 1b, 1c-d, 2, and paper I). As the figures showed, lines expected for $\ell < 8$ were often prominent in the F_{10} spectrum and exceeded the detection threshold 15 out of 17 times. Lines for higher ℓ were detected less often (11 of 21) but still more than the 32% random expectation. The weakness for higher ℓ is not

surprising since less information about smaller horizontal scales can make it up through the convection zone to affect the surface. For example, oscillation energy declines roughly as $(0.71\mathrm{R}/\mathrm{r})^{2\ell}$ for the higher ℓ modes. Evidence for $\ell = 1$ modes would require more space than is available here.

A standard solar model was used with the assumption that oscillations suffer significant reflection near 0.18R where the sound speed is anomalous. The assumption found support when values of ν_s near the expected 429 nHz gave good fits to the spectrum. Also, reflection of energy near 0.18R roughly doubles g-mode oscillation periods, partly explaining why their expected periods have not been detected (Palle 1991) even though their rotation rates are seen. Another implication follows from the ratio $\nu_d/\nu_s = 381/428.2$ determined in §3. This means that $\mathrm{J}/\mathrm{K} = 0.890$ and, by equation (3), the typical g-mode has a radial harmonic number $\mathrm{n} \cong 2.6\ell^*$ which is nearly in the asymptotic range. Finally, only the lowest degree g-modes ($\ell \leqslant 3$) deviate from equation (2) (table 1, paper I). No r-mode deviates except perhaps $\ell = 1$. Thus, second order terms neglected in deriving equation (2) are too small to be sensed in a half century of the 10.7 cm flux index except for the very lowest angular states.

REFERENCES

Basu, S., et al., 2000, ApJ, 535, 1078

Brun, A. S., Turck-Chieze, S., & Morel, P. 1998, ApJ, 506, 913

Christensen-Dalsgaard, J. & Berthomieu, G. 1991 in Solar Interior & Atmosphere, eds. A. N. Cox, W. C. Livingston, & M. S. Mathews (U. Arizona Press, Tucson)

Cowling, T. G. 1941, MNRAS, 101, 367

Cox, J. P. 1980, Theory of Stellar Pulsation (Princeton: Princeton U. Press)

Eff-Darwich, A., Korzennik, S. G., & Jimenez-Reyes, S. J. 2002, ApJ, 573 857

Guenther, D. B., Demarque, P., Kim, Y-C., & Pinsonneault, M. H. 1992, ApJ, 387, 372

Kosovichev, A. G., et al. 1997, Sol. Phys., 170, 43

Ledoux, P. ApJ, 114, 373

Palle, P. L. 1991, Adv. Space Res., 11, (4), 29

Provost, J., Berthomieu, G., & Rocca, A. 1981, A&A, 94, 126

Richard, O. & Vauclair, S. 1997, A&A, 322,671

Saio, H. 1982, ApJ, 256, 717

Smeyers, P., Craeynest, D., & Martens,, L. 1981, Ap&SS, 78, 483

Unno, W., Osaki, Y., Ando, H., Saio,H., & Shibahashi, H. 1989, Nonradial Oscillations of Stars (Tokyo: Univ. Tokyo Press)

Wolff, C. L. 1974, ApJ, 193, 721

Wolff, C. L. 1979, ApJ, 227, 943

Wolff, C. L. 1983, ApJ, 264, 667, (paper I)

Wolff, C. L. 2000, ApJ, 531, 591

Wolff, C. L. & Hoegy, W. R. 1989, Solar Phys., 123, 7

Table 1. CORIOLIS EFFECT ON g-MODES

ℓ	n	J/K	ℓ	n	J/K
3	5	.7142	5	20	.9364
3	10	.9090	5	25	.9549
3	15	.9526	10	10	.5236
3	20	.9699	10	15	.7430
5	5	.4556	10	20	.8372
5	6	.5738	10	25	.8803
5	8	.7243	15	15	.5576
5	10	.8087	15	20	.7109
5	15	.9020	15	25	.7924

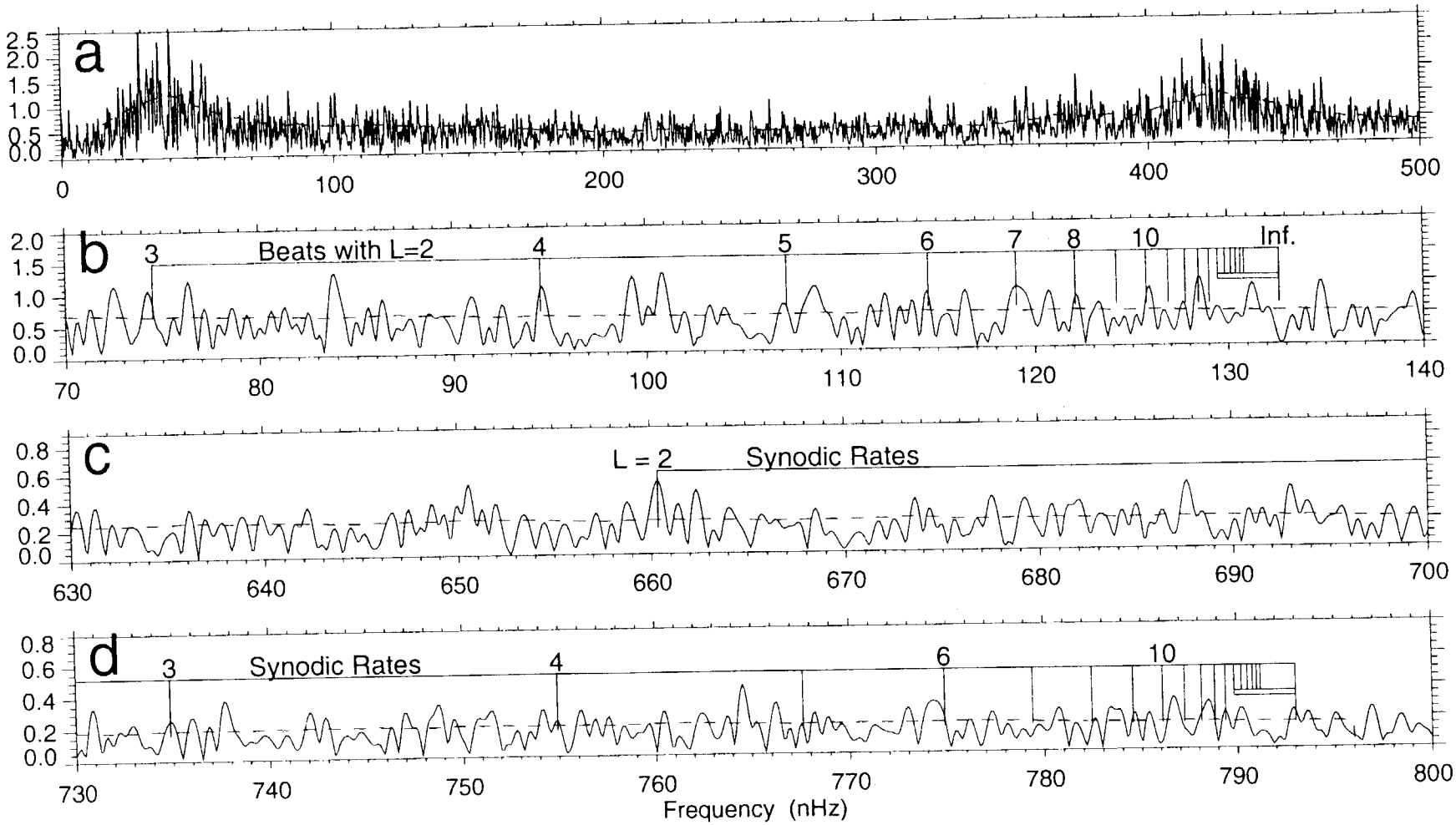

Fig. 1 -- The spectrum of a half century of the 10.7 cm solar radio flux index and expanded segments. (a) The mound peaking at 430 nHz is associated with solar rotation rates and the rise below 60 nHz may be due to g-mode beats. (b) The sequence of rotational beats between the L = 2 g-mode and modes of higher L is strongly detected in the spectrum up to L = 8 and probably beyond. The detection threshold (dashed curve) lies above 2/3 of the spectrum. (c & d) The corresponding rates at which the g-mode hot longitudes face Earth are also detected, but less firmly because they are weaker, as expected. The 10.7 cm record is too short to resolve any mode for L > 14, indicated by the flat rectangle ending at L = infinity.

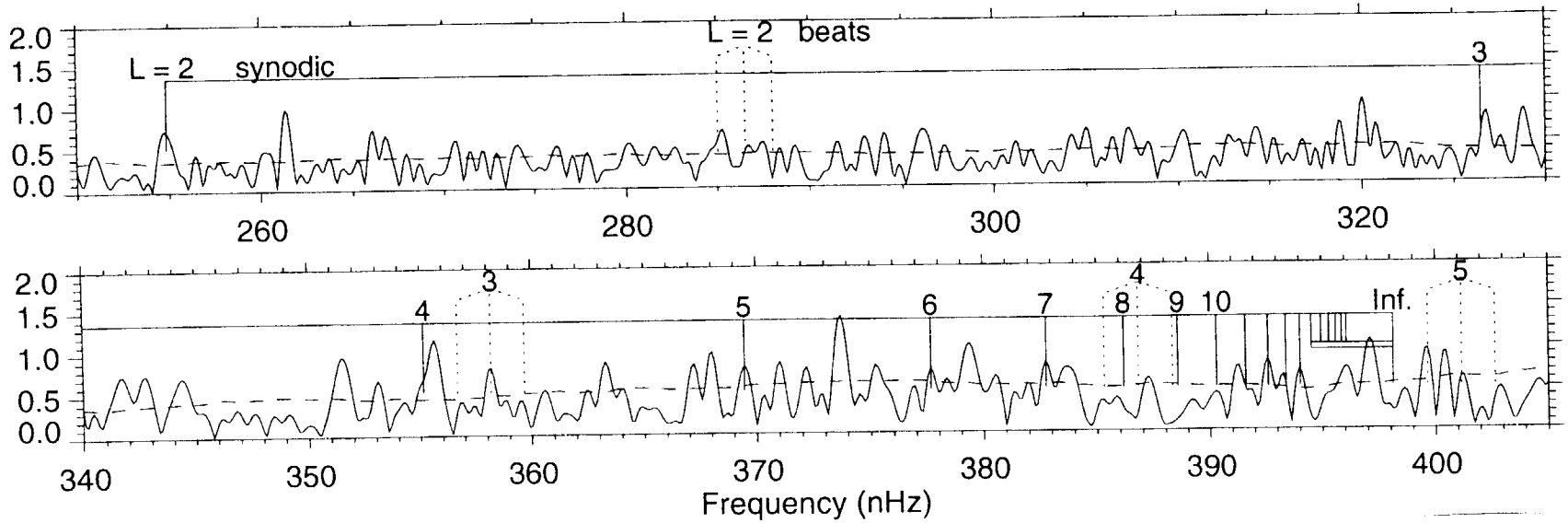

Fig. 2-- Part of the same observed spectrum on Figure 1. Theoretical lines are now the synodic rotation rates of r-modes. Again, all low angular harmonics are detected as well as some others up to the resolution limit. The L = 9 case suffers interference from one of the dotted triplets located where r-mode beats (and aliases) with the L = 1 modes should be located.